Proceedings of the 2006 IEEE International Conference on Robotics and Automation
Orlando, Florida - May 2006

Towards Automated Gait Generation for Dynamic Systems with Non-holonomic Constraints

Elie Shammas Howie Choset Alfred Rizzi
Carnegie Mellon University, Pittsburgh, PA 15213, U.S.A.
Email: elie.shammas@cmu.edu, choset@cs.cmu.edu, arizzi@cs.cmu.edu

***Abstract*— In this paper we generate gaits for dynamics systems that are subject to non-holonomic velocity constraints. These systems are referred to as mixed non-holonomic systems. The motion of such systems is governed by both the non-holonomic constraints acting on the system and a system of differential equations constraining the evolution of generalized momentum. We propose a method that utilizes both governing motions, that is, satisfying all the constraints and instantaneously conserving momentum along un-restricted directions, to generate gaits for systems like the snakeboard, which belongs to the family of mixed non-holonomic systems. We accomplish this by defining a new scaled momentum variable. This scaled momentum allows us to easily explore the design of gaits that causes momentum to evolve such that a desired non-trivial motion results.**

I. Introduction

In this paper we develop a general and intuitive formulation for the gait generation problem that applies to a broad class of mechanical systems. We classify mechanical systems into three categories: *purely mechanical systems*, that is, systems whose motion is governed solely by the conservation of momentum; *principally kinematic systems*, that is, systems whose motion is governed solely by the existence of a set of independent non-holonomic constraints that fully constrain the system's velocity; and *dynamic systems with non-holonomic constraints*, that is, systems whose motion is governed by a non-holonomic set of constraints as well as generalized momentum being constrained by a set of differential equations.

In this paper we generate gaits for dynamic systems with non-holonomic constraints which is the most general of the three types of systems described above. We shall refer to such systems as *mixed systems* throughout this paper. Recall that the *configuration space* of mechanical systems can be naturally divided into two subspaces, the *fiber space* which represents the position of the system with respect to a fixed inertial frame and the *base space* which represents the internal degrees of freedom of the robot, that is the robot's shape. Since we assume control solely over the base variables, the mechanical systems we deal with are necessarily *under-actuated*. The snakeboard shown in Fig. 1 is an example of such a system. We generate gaits to move the snakeboard in the plane along a specified fiber direction by coordinating its wheels and rotor rotations, that is, the snakeboard's base variables.

What is interesting about mixed systems is that the set of non-holonomic velocity constraints do not completely constrain the system's velocity as is the case for principally kinematic systems. In other words, for mixed systems the velocity constraints do not completely span the fiber space. Thus, there must exist unrestricted directions along which the constraints do not act. For motions along these directions the generalized momentum is governed by a first order differential equation that depends solely on the base variables. For the snakeboard, rotations about the point of intersection of the wheel axes are allowable motions for which momentum is instantaneously conserved.

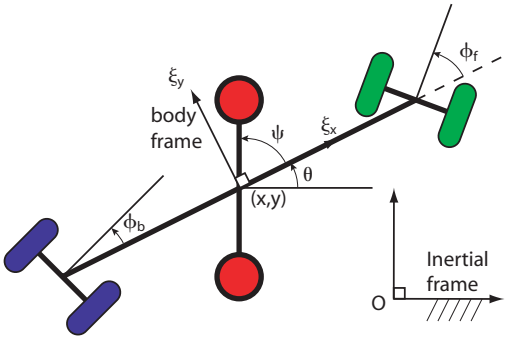

Fig. 1. A schematic of the snakeboard denoting its five configuration variables $(x, y, \theta, \alpha_1, \alpha_2)$. The snakeboard is a simple mixed system that was extensively studied in the literature. In this paper we apply our gait analysis and generate an extensive family of gait for this system.

Our goal is to design cyclic curves in the base space, which after a complete cycle, produce a desired motion in the fiber space, effectively moving the robot to a new desired position. Therefore, ideally we would like to have a "relation" between the fiber and base variables to study the effect of any base motion on the position of the robot. We take recourse to mechanics of locomotion which provides such a relation. This relation describes position velocities as seen from the body-fixed frame as a function of base configurations, base velocities, and generalized momentum, the latter of which is governed by a set of differential equations. Manipulating this relation gives us an equation that allows us to examine the position change due to any closed motion in the base space. This is one of this paper's major contributions. Specificaly, for a family of parameterizable gaits, we can systematically design all the parameters of the motion such as frequencies and magnitudes, and eliminate the need for designer's intuition in finding and tuning these parameters. Moreover, our approach applies to all three type of mechanical systems.

II. Prior Work

Early gait generation work was biologically inspired as was the case of Hirose's locomoting snake robots [5], where they observed how real snakes locomote and implemented the same shape changes on a snake robots. The shape changes followed what they defined as the *serpenoid* curve.

Ostrowski et. al. [13], on the other hand, took advantage of the idea of translational symmetry from physics, which allowed them to project the entire dynamics of the system onto the base space. Moreover, by representing the system dynamics with respect to a body-fixed frame, a relation between fiber velocity on one hand and base and momentum variables on the other was devised. This decoupling relation is referred to as the *reconstruction equation* which allowed for the system's dynamics to be represented as an affine non-linear control system. Then by taking recourse to geometric control theory, the degree of Lie brackets of the control vector fields required to span the fiber velocities was related to the frequencies of the sinusoidal inputs of the base variables [13]. Using this approach, they intuitively developed and then analyzed gaits for principally kinematic and mixed systems. In fact, they generated gaits for the snakeboard (Fig. 1). This approach was applicable to sinusoidal inputs where only the gait frequencies were determined, however, the magnitudes were empirically derived to produce the desired motion.

The work done by Bullo et. al. on kinematic reduction of simple mechanical systems is closely related to our work [3]. Even though, their main contribution is actually the kinematic reduction of simple mechanical systems and analyzing the controllability of such systems, they did generate gaits for certain examples such at the snakeboard with we are analyzing in this paper, [2]. They generated gaits by restricting themselves to using kinematic gaits, i.e., gaits that do not change the generalized momentum of the system. We shall see later in the paper how our approach yields structurally similar kinematic gaits as a special case. For further reading about similar works, the reader is referred to [1], [6], [9], [13], [14], and [18].

Another entirely different approach was presented by Mukherjee et. al. [8], [10], [11] and by Yamada [19]. They generated gaits for the rolling disk (principally kinematic system) and space robots (purely mechanical systems) by relating position change to a volume integral of a well-defined function. Shammas et. al. independently developed a similar but more general approach and generated gaits for two types of mechanical system: purely mechanical systems in [16] and for principally kinematic systems in [15]. Moreover, their work presents an optimality analysis for gait generation.

III. Background Material

In this section we rigorously define *mixed systems* and several other technical terms that are needed for our gait generation technique.

A. Configuration manifolds

We remind the reader that a configuration uniquely specifies the location in two or three dimensions of each physical point of the mechanism or robot. For a robot that is made up of many rigid bodies, both fiber variables which describe the robot's position with respect to an inertial frame, and base variables which describe the robot's internal angles, are needed to specify the robot's configuration. Moreover, the configuration space of mechanical systems is usually denoted by $Q = G \times M$ whose structure is a *trivial fiber bundle*[1] where G is an l-dimensional fiber space with a Lie group structure and M is an m-dimensional base space. Hence, Q is n-dimensional with $n = l + m$.

B. Mixed systems

Non-holonomic constraints are constraints that act on configuration velocities and are, by definition, not integrable. Such constraints are typically seen in mechanical systems with wheels or rolling elements. The assumption that wheels can not slide sideways or slip while rolling give rise to a non-holonomic set of constraints. In this paper we will assume that a non-holonomic set of k constraints can be written in a Pfaffian form

$$\omega(q) \cdot \dot{q} = 0, \tag{1}$$

where $\omega(q)$ is a $k \times n$ matrix describing the constraints and $\dot{q}$ represents an element in the tangent space of the n-dimensional configuration manifold Q. While principally kinematic systems have "enough" linearly independent non-holonomic constraint to completely specify fiber motions as a function of the base variables, mixed systems do not have "enough" non-holonomic constraints to do this. The implications is that for any configuration of the robot, there exist fiber velocities that are perpendicular to all of the constraints. Moreover, the set of non-holonomic constraints need to be invariant with respect to the Lie group action associated with the fiber space.

Definition 3.1: Given a mechanical system that has a configuration space with trivial principal fiber structure, $Q = G \times M$ and is subjected to k non-holonomic constraints, $\omega(q) \cdot \dot{q} = 0$, then a system is said to be *mixed* if

- $0 < k < l$ (# constraints less than dim of fiber space),
- $\det(\omega(q)) \neq 0$ (linear independence),
- $\omega(q) \cdot \dot{q} = \omega(\Phi_g(q)) \cdot T_g\Phi_g(\dot{q}) = 0$ (invariance),

where Φ_g and $T_g\Phi_g$ are the Lie group's action and lifted action, respectively.

C. Mechanics of locomotion

Now we borrow some well known results from the mechanics of locomotion, [7], which we shall build upon for our own gait generation techniques. For a mixed system, the system's configuration velocity expressed in body coordinates, ξ, is given by the *reconstruction* equation

$$\xi = -\mathbf{A}(r)\dot{r} + \Gamma(r)p \tag{2}$$

[1]Please refer to [1] and [6] for an extensive study of simple mechanical systems and their configuration space structure.

where $\mathbf{A}(r)$ is an $l \times m$ matrix denoting the local form of the mixed non-holonomic connection, $\Gamma(r)$ is an $l \times (l-k)$ matrix, and p is the generalized non-holonomic momentum, that is, the momentum along the allowable directions of motions which are orthogonal to all constraints. Gait generation for systems where the second term in (2) vanishes have been studied in [16] for purely mechanical systems where the momentum is zero for all time and [15] for principally kinematic systems where momentum it totally annihilated by the constraints.

Moreover, for systems with a single generalized momentum variable[2], its evolution is governed by the following differential equation

$$\dot{p} = p^T \sigma_{pp}(r) p + 2p^T \sigma_{p\dot{r}}(r)\dot{r} + \dot{r}^T \sigma_{\dot{r}\dot{r}}(r)\dot{r} \tag{3}$$

where the σ's are matrices of appropriate dimensions whose components depend solely on the base variables. Next we will utilize both (2) and (3) and rewrite them in appropriate forms that will help us generate gaits.

IV. Scaled Momentum

In this section we will manipulate (3) to a more manageable form which will alow us to generate gaits. At this point we will limit ourself to systems that have one less velocity constraint than the dimension of the fiber space, i.e., $l-k=1$. This leaves us with only one generalized momentum variable and forces the term $\sigma_{pp}(r) = 0$ in (3) as was explained in [12]. First order differential equations theory confirms that an integrating factor[3], $h(r)$, exists for (3). Now, we define the scaled momentum as $\rho = h(r)p$, then (2) and (3) reduce to

$$\begin{aligned} \xi &= -\mathbf{A}(r)\dot{r} + \bar{\Gamma}(r)\rho, & (4)\\ \dot{\rho} &= \dot{r}^T \bar{\Sigma}(r)\dot{r}. & (5) \end{aligned}$$

where $\bar{\Gamma}(r) = \Gamma(r)/h(r)$ and $\bar{\Sigma}(r) = \frac{1}{2}h(r)\sigma_{\dot{r}\dot{r}}(r)$. Now that we have written the reconstruction and momentum evolution equations, (2) and (3), in our simplified forms shown in (4) and (5), we are ready to generate gaits by studying and analyzing the three terms, $\mathbf{A}(r)$, $\bar{\Gamma}(r)$, and $\bar{\Sigma}(r)$.

V. Gait analysis

In this paper, we define a *gait* as a closed curve, γ, in the base space, M, of the robot. We require that our gaits be cyclic, that is, the system will retain its original shape after each period of time; moreover, we require γ to be continuous. Having written the body representation of a configuration velocity in a simplified manner as seen in (4), we integrate this equation to get a position change. Define ζ as the integral of ξ, that is, $\dot{\zeta} = \xi$, then integrating the i-th row of (4) with respect to time we get

$$\begin{aligned} \Delta\zeta^i &= \int_{t_0}^{t_1} \dot{\zeta}^i dt = \int_{t_0}^{t_1} \xi^i dt \\ &= \int_{t_0}^{t_1} \left(-\sum_{j=1}^{m} \mathbf{A}_j^i(r)\dot{r}^j + \sum_{j=1}^{l-k} \bar{\Gamma}_j^i(r)\rho^j \right) dt \\ &= -\oint_\gamma \sum_{j=1}^{m} \mathbf{A}_j^i(r) dr^j + \int_{t_0}^{t_1} \sum_{j=1}^{l-k} \bar{\Gamma}_j^i(r)\rho^j dt \\ &= \underbrace{\int\int_\Gamma \sum_{o,j=1,o<j}^{m} \left(\bar{\mathbf{A}}_{oj}^i(r) \right) dr^o dr^j}_{I^{GEO}} \\ &\quad + \underbrace{\int \sum_{j=1}^{l-k} \left(\bar{\Gamma}_j^i(r) \int \left(\dot{r}^T \bar{\Sigma}(r)\dot{r} \right)^j dt \right) dt}_{I^{DYN}} \end{aligned} \tag{6}$$

Here, we used Stokes' theorem to transform the first component of the integrand above, the line integral of the one-from $\mathbf{A}_j^i(r)dr^j$, to a volume integral of a two-form. We label this term at I^{GEO} since this integral computes the *geometric phase* shift due to any gait γ. Moreover, we refer to the integrands of the volume integral, $\bar{\mathbf{A}}_{oj}^i(r)$, as *height functions*. We shall see later, that for mechanical systems with a two-dimensional base space, the geometric phase shift, I^{GEO}, is literary the volume under the graph of the height function, $\bar{\mathbf{A}}^i(r)$, which is bounded by the gait, γ. Thus, by analyzing these height functions, we can intuitively design curves, or gaits, in the base space that yield non-zero volume under a specified height function, thus, moving the mechanical system along a desired direction.

As for the second set of integrals I^{DYN}, in general we can not equate those to volume integrals. Instead, by analyzing the values of $\bar{\Gamma}^i$ and $\bar{\Sigma}$, we are able to design gaits that are guaranteed to yield a non-zero I^{DYN}. We do so by easily designing gaits which ensure that the scaled momentum is sign definite, then by analyzing the *gamma functions*, $\bar{\Gamma}^i$, we are able to select the gaits that ensure I^{DYN} along a specified direction is non-zero. We call the second integral in (6) I^{DYN} since it computes the *dynamic phase* shift due to the proposed gait.

Thus far, we have explained how each of the two components of the reconstruction equation (6) can contribute motion along a specified direction. Next, we define a partition on the space of possible gaits such that either I^{GEO} or I^{DYN} are non-zero along a specified fiber direction. This partition yields the following two types of gaits.

A. Purely kinematic gaits

Purely kinematic gaits are gaits for which $I^{DYN} = 0$. The simplest set of gaits that set $I^{DYN} = 0$ are gaits that have $\rho = 0$ for all time which means that $p = 0$ for all time as well. Thus, for purely kinematic gaits position change is equal to I^{GEO} only. Shammas et. al. in [15] and [16] have

[2]For systems with more than one generalized momentum variables, (3) will be a systems of differential equations involving tensor operations. Please refer to to [1], [6], [9], and [13] for more details.

[3]Integrating factors allow us to rewrite first order differential equations of the form $dp/dt = f(r, p, \dot{r})$ as $d(h(r)p)/dt = \bar{f}(r, \dot{r})$, [17].

studied extensively how to generate optimal gaits for systems whose change of position is equal to solely I^{GEO}. We use the same approach to do volume integration analysis and generate these kinematic gaits. Note, these gaits are structurally similar to gaits proposed by Bullo in his kinematic reduction of mechanical systems in [2] as it will be clear when we examine the snakeboard example.

To summarize, we generate purely kinematic gaits by first solving for $\rho = 0$ in (5). This will define vector field over the base space whose integral curves are candidate purely kinematic gaits. Then, we analyze the height functions and construct gaits from pieces of integral curves that enclose a non-zero volume under the desired height function.

B. Purely dynamic gaits

As the name suggests these are gaits that produce motion solely due to the dynamic phase shift, that is, $I^{GEO} = 0$ while $I^{DYN} \neq 0$. These gaits are relatively easy to design since these are gaits that enclose no "volume" in the base space. A simple solution for a possible candidate gaits would be to ensure that a gait retraces the same curve in the second half cycle of the gait but in opposite direction. We propose the following purely dynamic families of gaits

$$r_1 = a_0 + \sum_{i=1}^{n} a_i \left(f(t)\right)^i \tag{7}$$

$$r_2 = f(t) \tag{8}$$

where $f(t) = f(t+\tau)$ is a periodic real function and a_i's are real numbers. For such gaits, we can verify that they will enclose zero area in the base space and we can ensure that the scaled momentum variable is sign definite. Then by analyzing the gamma functions in (4) we pick the candidate gaits which ensure that I^{DYN} has a non-zero value along the desired fiber direction. Next, we analyze the snakeboard example and generate the above two types of gaits for it.

VI. Example: Snakeboard

A schematic of the snakeboard, seen in Fig. 1, denotes the system's configuration variable, $q = (x, y, \theta, \phi, \psi)$[4]. Moreover, let the mass and inertia of the entire system be denoted by M and J, respectively. The rotor and wheel inertias are denoted by J_r and J_w, respectively. Then setting $J + J_r + 2J_w = ML^2$ for simplification, we can compute the reduced Lagrangian and the non-holonomic constraints written in body coordinates as

$$l(\xi, r, \dot{r}) = \frac{M(\xi_x^2 + \xi_y^2 + \xi_\theta^2) + J_r(2\xi_\theta\dot{\psi} + \dot{\psi}^2) + 2J_w\dot{\phi}^2}{2},$$

$$0 = \underbrace{\begin{pmatrix} -\sin\phi & \cos\phi & L\cos\phi \\ \sin\phi & \cos\phi & -L\cos\phi \end{pmatrix}}_{\bar{\omega}_\xi} \begin{pmatrix} \xi_x \\ \xi_y \\ \xi_\theta \end{pmatrix}. \tag{9}$$

[4]We assume that $\phi = \phi_b = -\phi_f$.

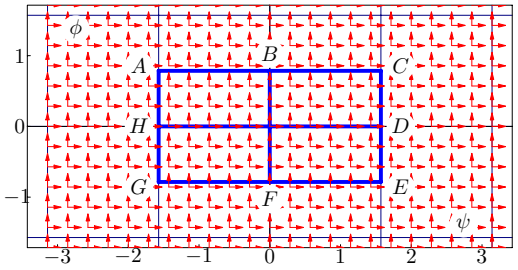

Fig. 2. The vector fields defined over the base space of the snakeboard, (ϕ, ψ)), whose integral curves are purely kinematic gaits. The solid lines indicate our proposed purely kinematic gaits for the snakeboard.

Then we can compute the generalized non-holonomic momentum p using the equation $p = \frac{\partial l}{\partial \xi}\bar{\Omega}^T$, where $\bar{\Omega}^T$ is a basis of $\mathcal{N}(\bar{\omega}_\xi)$, the null space of $\bar{\omega}_\xi$.

$$p = ML(\xi_x \cot\phi + L\xi_\theta) + J_r\dot{\psi}. \tag{10}$$

Now we use (9) and (10) to compute the reconstruction and the momentum evolution equations

$$\xi = -\begin{pmatrix} 0 & \frac{J_r \sin 2\phi}{2ML} \\ 0 & 0 \\ 0 & \frac{J_r \sin^2\phi}{ML^2} \end{pmatrix} \begin{pmatrix} \dot{\psi} \\ \dot{\phi} \end{pmatrix} + \begin{pmatrix} \frac{\sin 2\phi}{2ML} \\ 0 \\ \frac{\sin^2\phi}{ML^2} \end{pmatrix} p, \tag{11}$$

$$\dot{p} = -p\dot{\phi}\cot\phi + J_r\dot{\psi}\dot{\phi}\cot\phi. \tag{12}$$

Then we compute the integrating factor for (12) such that $h(\psi, \phi) = \exp(\int \cot\phi\dot{\phi}dt) = \sin\phi$. Using the new scaled momentum, we rewrite (4) and (5) to get

$$\xi = -\begin{pmatrix} 0 & \frac{J_r \sin 2\phi}{2ML} \\ 0 & 0 \\ 0 & \frac{J_r \sin^2\phi}{ML^2} \end{pmatrix} \begin{pmatrix} \dot{\psi} \\ \dot{\phi} \end{pmatrix} + \begin{pmatrix} \frac{\cos\phi}{ML} \\ 0 \\ \frac{\sin\phi}{ML^2} \end{pmatrix} \rho, \tag{13}$$

$$\dot{\rho} = J_r\dot{\psi}\dot{\phi}\cos\phi. \tag{14}$$

Note that the local form of the mixed connection remains unchanged as we rewrite the equations in terms of the new scaled momentum ρ. Now, we are ready to design gaits but first we have to integrate both (13) and (14), to arrive at

$$\Delta\zeta_x = \int\int \overbrace{\frac{J_r\cos 2\phi}{ML}}^{F_1} d\phi d\psi + \int (\overbrace{\frac{\cos\phi}{ML}}^{G_1} \int \overbrace{\frac{J_r\dot{\psi}\dot{\phi}}{\sec\phi}}^{\dot{\rho}} dt)dt,$$

$$\Delta\zeta_y = \int\int \overbrace{0}^{F_2} d\phi d\psi + \int (\overbrace{0}^{G_2} \int \overbrace{\frac{J_r\dot{\psi}\dot{\phi}}{\sec\phi}}^{\dot{\rho}} dt)dt,$$

$$\Delta\zeta_\theta = \int\int \overbrace{\frac{J_r\sin 2\phi}{ML^2}}^{F_3} d\phi d\psi + \int (\overbrace{\frac{\sin\phi}{ML^2}}^{G_3} \int \overbrace{\frac{J_r\dot{\psi}\dot{\phi}}{\sec\phi}}^{\dot{\rho}} dt)dt,$$

where F_i's and G_i's are the respective height and gamma functions for the snakeboard. The first column of Fig. 3 and

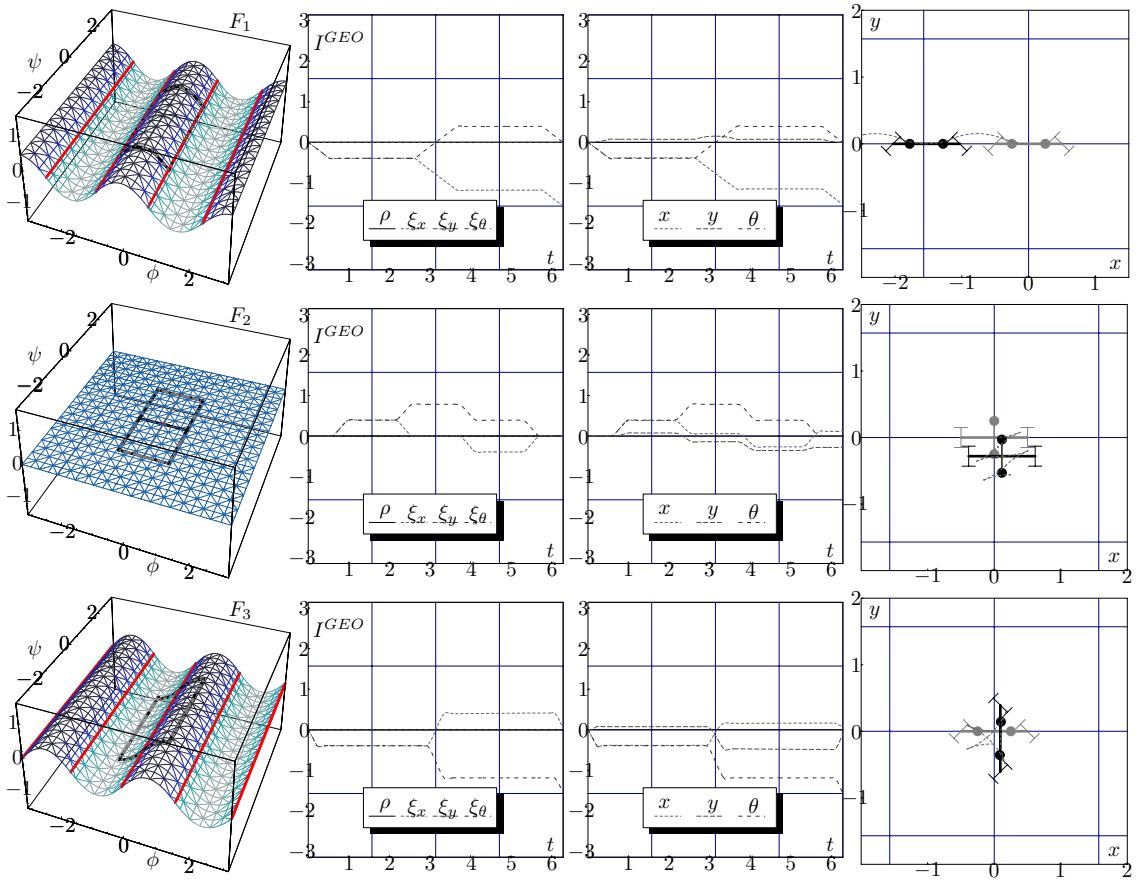

Fig. 3. Numerical simulation of three *purely kinematic* gaits, each row corresponds to one of the gaits. In the first column we superimposed all three gaits on top of all three *height functions*, but for each row we highlighted one gait with a dark solid color. The second column depicts the values of I^{GEO} along the $(\xi_x, \xi_y, \xi_\theta)$ directions as well as the scaled momentum variable, ρ. The third column depicts the fiber variables, (x, y, θ), versus time while the last column depicts that actual motion of the snakeboard due to each of the three purely kinematic gaits. Observe that for all three gaits, $\rho = 0$ for all time and $\xi_y = 0$ since the second height function is identically zero all over the base space.

Fig. 4 depict the snakeboard's height and gamma functions, respectively. Note that the second height and gamma functions are identically zero; moreover, the other two height and gamma functions are independent of the rotor angle ψ which explains the extruded shape of the graphs.

A. *snakeboard example: purely kinematic gaits*

For kinematic gaits, we need to set $\rho = 0$. This is easily done by considering (14). The simplest solution for which $\rho = 0$ is the set of gaits that satisfy the condition $\{\dot{\phi} = 0$ or $\dot{\psi} = 0\}$. The integral curves defining purely kinematic gaits for the snakeboard are horizontal and vertical lines, that is, the designed gaits should only move along one base variable at a time. We have plotted the above vector fields over the base space as shown in Fig. 2. Thus, any part of an integral curve of the above vector fields could be used to construct a purely kinematic gait for the snakeboard. Note that, these vector fields serve the same purpose of the decoupling vector fields described by Bullo in [3]. This explains the similarity of our purely kinematic gaits to those proposed by Bullo.

Analyzing the height functions of the snakeboard, we can can easily design the following purely kinematic gaits which flow along the integral curves depicted in Fig. 2

$$\begin{aligned} \gamma_1^k &= A - C - E - G - A \\ \gamma_2^k &= A - B - F - E - C - B - F - G - A \\ \gamma_3^k &= A - C - D - H - G - E - D - H - A \end{aligned}$$

The three gaits are depicted in Fig. 3. For instance, consider the first gait, γ_1^k, which is a rectangular gait centered at the origin of the base space. All the sides of the rectangle are integral curves, thus, for this gait, $\rho = 0$. Moreover, this gait envelopes a non-zero volume solely under the first height function, as shown in the first plot of the first row of Fig. 3. This implies that we expect $\Delta\zeta_x \neq 0$ while $\Delta\zeta_y = \Delta\zeta_z = 0$ as shown in the second plot of the first row of Fig. 3. Moreover, we numerically simulated the above gait and plotted the fiber variables, (x, y, θ), versus time. We can see that this specific

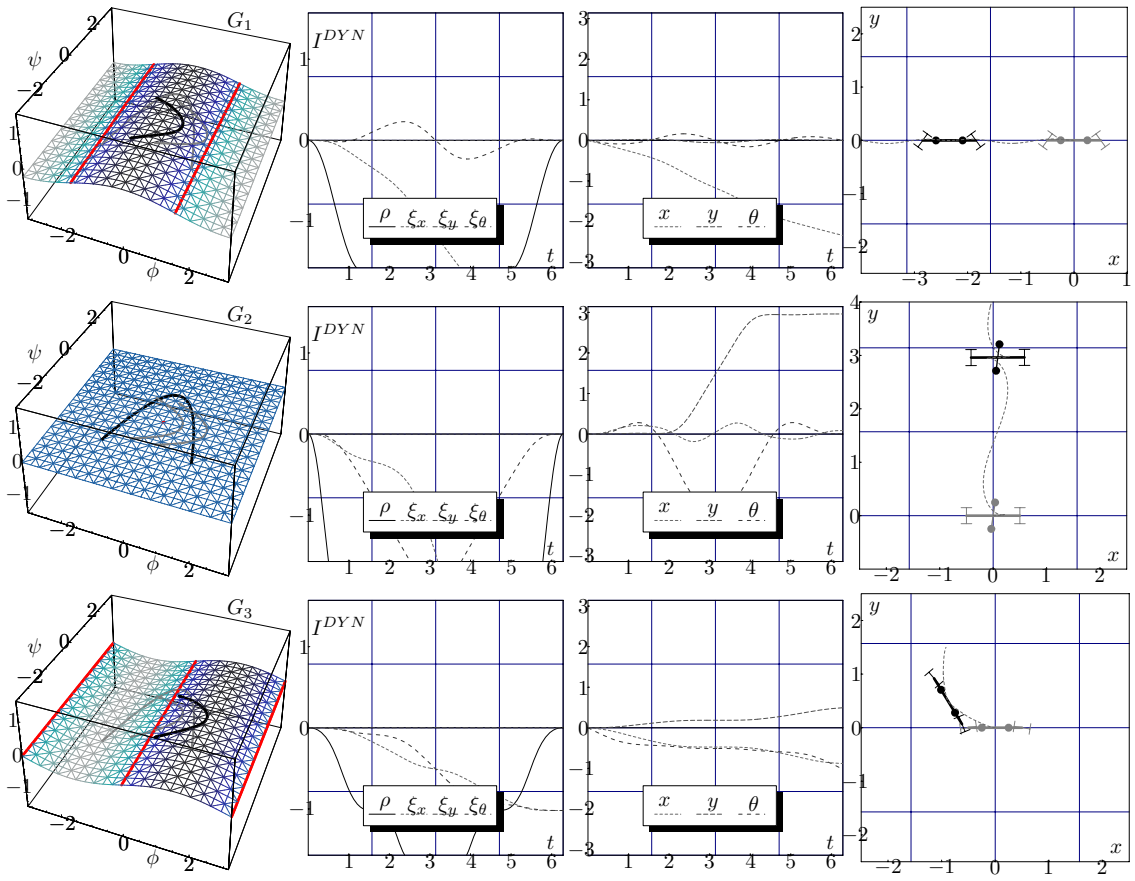

Fig. 4. Numerical simulation of three *purely dynamic* gaits, each row corresponds to one of the gaits. In the first column we superimposed all three gaits on top of all three *gamma functions*, but for each row we highlighted one gait with a dark solid color. The second column depicts the values of I^{DYN} along the $(\xi_x, \xi_y, \xi_\theta)$ directions as well as the scaled momentum variable, ρ. The third column depicts the fiber variables, (x, y, θ), versus time while he last column depicts that actual motion of the snakeboard due to each of the three purely dynamic gaits. Observe that the scaled momentum is sign definite, $\rho \leq 0$, for all three gaits.

gait translates the snakeboard solely along the x direction as shown in the last two plots of the first row of Fig. 3.

Similarly, the second row in Fig. 3 depict a gait that encloses a zero volume under all height functions. However, it has been our experience that such gaits yield motion along the global y-direction[5]. Remember, that we are integrating the body representation of the systems velocity, so even though we have zero volume under all height functions, we might still have a non-zero global position change. Finally, the third row of Fig. 3 depicts a gait that encloses a non-zero volume only under the third height function. Indeed, this gait yields a pure global rotation of the snakeboard.

B. snakeboard example: purely dynamic gaits

As for purely dynamic gaits, first we ensure that the gaits belong to the candidate family of gaits described in (7) and (8). For simplicity, we let one of the base variables be a sinusoidal input. This assumption is not critical for our gait generation, but we used it to simplify the numerical simulation of the proposed gaits. Now consider the following three purely dynamic gait.

$$\begin{aligned}
\gamma_1^d \quad : \quad & \phi = \tfrac{\pi}{5}(1 - 2\sin^2(t)) \\
& \psi = \tfrac{\pi}{3}\sin(t) \\
\gamma_2^d \quad : \quad & \phi = \tfrac{5\pi}{11}\sin(t) \\
& \psi = \tfrac{5\pi}{11}(1 - 2\sin^2(t)) \\
\gamma_3^d \quad : \quad & \phi = \tfrac{\pi}{5}(1 - 2\sin^2(t)) + \tfrac{\pi}{4} \\
& \psi = \tfrac{\pi}{3}\sin(t)
\end{aligned}$$

All three gaits are superimposed over the gamma functions as shown in the first column of Fig. 4. We can verify that for all three gaits, the scaled momentum $\rho \leq 0$ for all time, that is, it is sign definite as shown in the second column of Fig. 4. Moreover, note that all three gaits enclose zero area in the base space, since the gaits retrace the same curves in the second

[5]Note that for all three purely kinematic gaits $I^{DYN} = 0$ along ξ_y for all time since the second height function is identically zero as shown in the first plot of the second row of Fig. 3.

half cycle of each gait. Thus, for all three gaits, $I^{GEO} = 0$ for all time. Thus, to design gaits we need to analyze the gamma functions and place the curves accordingly to produce a non-zero specified I^{DYN}.

For instance, consider the first purely dynamic gait, γ_1^d depicted in the first row of Fig. 4. This gait is located close to the origin of the base space, where only the first gamma function is positive. Moreover, note that this gait is centered about the line $\phi = 0$ and that the third gamma function is odd about this specific line. Thus, we can conclude that this gait will yield a non-zero I^{DYN} only along the ξ_x direction as shown in the second plot of the first row of Fig. 4. We numerically simulate this gait and indeed it translates the snakeboard along the x direction as shown in the last two plots of the first row of Fig. 4.

Similarly, we designed the other two gaits, γ_2^d and γ_3^d to translate the snakeboard along the y direction and rotate it as respectively shown in the second and third rows of Fig. 4.

VII. Discussion

In this paper, we proposed two types of gaits, purely kinematic and purely dynamic gaits. These gaits produce motion of a mechanical system exclusively due either the geometric or dynamic phase shift. Currently, we are working on a third type of gaits, *kino-dynamic gait*, which utilizes both the geometric as well as the dynamic phase shift to simultaneously produce motion with relatively larger magnitudes.

Moreover, in this paper, we analyzed a well know mechanical system, the snakeboard. Even though the snakeboard is representative of a rather large family or mechanical systems, dynamic systems with non-holonomic constraints, this particular system is rather simple which lead to the relatively simply expressions of the reconstruction and momentum evolution equation. Recently, we have defined a novel mechanical system, the *variable inertia snakeboard*, which we consider to be a generalization of the snakeboard studied in the prior work and this paper. Indeed, this novel system is not as simple as the original snakeboard, yet our gait generation techniques are still applicable which proves the generality of our approach.

VIII. Conclusion and Future Work

In this paper, we studied mixed non-holonomic systems and designed two families of gaits, purely kinematic and purely dynamic gaits, for the snakeboard. Even though our proposed gaits can be found in the prior work, our work unifies prior methods (kinematic reduction and Lie bracket analysis) under one generation technique. Moreover, our technique has better control over all parameters of the suggested gaits, which allows for optimality analysis and reduces the need for deeper intuition to manually set these parameters.

This paper constitutes a first attempt at designing gaits for mixed systems. We do acknowledge the fact that the snakeboard is a fixed inertia system which not only simplifies the mathematical expression of various terms we analyzed but also simplifies finding purely kinematic gaits. We are still in the process of studying mixed systems and designing gaits for more involved mixed systems such as the variable inertia snakeboard. Thus far, we have discovered that most of the analysis presented in this paper still holds; the main difference is in actually designing the purely kinematic gaits. This process is indeed more involved and we shall address it in our future work.

Finally, we would like to relax some of the assumptions in this paper. For example, we would like to investigate what happens when more than one non-holonomic generalized momentum variable exists and how will this affect the existence of integrating factors. We would also like to investigate systems that have the geometric phase shift identically zero by definition. The robo-Trikke introduced by Chitta *et.al.* in [4] is such a system. This particular system has a one-dimensional base space, hence, all possible gaits are necessarily purely dynamic. Thus, we would like to apply our purely dynamic gait analysis on such systems.

References

[1] A. Bloch. *Nonholonomic Mechanics and Control*. Springer Verlag, 2003.

[2] F. Bullo and A. D. Lewis. Kinematic Controllability and Motion Planning for the Snakeboard. *IEEE Transactions on Robotics and Automation*, 19(3):494–498, 2003.

[3] F. Bullo and A. D. Lewis. *Geometric Control of Mechanical Systems: Modeling, Analysis, and Design for Simple Mechanical Control Systems*. Springer, 2004.

[4] S. Chitta, P. Cheng, E. Frazzoli, and V. Kumar. Robotrikke: A novel undulatory locomotion system. In *IEEE International Conference on Robotics and Automation*, 2005.

[5] S. Hirose. *Biologically Inspired Robots (Snake-like Locomotor and Manipulator)*. Oxford University Press, 1993.

[6] J. Marsden. *Introduction to Mechanics and Symmetry*. Springer-Verlag, 1994.

[7] J.E. Marsden, R. Montgomery, and T.S. Ratiu. Reduction, symmetry and phases in mechanics. *Memoirs of the American Mathematical Society*, 436, 1990.

[8] R. Mukherjee and D.P. Anderson. Nonholonomic motion planning using stoke's theorem. In *IEEE International Conference on Robotics and Automation*, 1993.

[9] R. M. Murray and S. S. Sastry. Nonholonomic motion planning: Steering using sinusoids. *IEEE T. Automatic Control*, 38(5):700 – 716, May 1993.

[10] Y. Nakamura and R. Mukherjee. Nonholonomic path planning of space robots. In *IEEE International Conference on Robotics and Automation*, 1989.

[11] Y. Nakamura and R. Mukherjee. Nonholonomic path planning of space robots via a bidirectional approach. In *IEEE Transactions on Robotics and Autmation*, volume 7, pages 500–514, 1991.

[12] J. Ostrowski. *The Mechanics of Control of Undulatory Robotic Locomotion*. PhD thesis, California Institute of Technology, 1995.

[13] J. Ostrowski and J. Burdick. The mechanics and control of undulatory locomotion. *International Journal of Robotics Research*, 17(7):683 – 701, July 1998.

[14] J. Ostrowski, J. Desai, and V. Kumar. Optimal gait selection for nonholonomic locomotion systems. *International Journal of Robotics Research*, 2000.

[15] E. Shammas, H. Choset, and A. Rizzi. Natural gait generation techniques for principally kinematic mechanical systems. In *Proceedings of Robotics: Science and Systems*, Cambridge, USA, June 2005.

[16] E. Shammas, K. Schmidt, and H. Choset. Natural gait generation techniques for multi-bodied isolated mechanical systems. In *IEEE International Conference on Robotics and Automation*, 2005.

[17] M. Tenenbaum and H. Pollard. *Ordinary Differential Equations*. Courier Dover Publications, 1985.

[18] G. Walsh and S. Sastry. On reorienting linked rigid bodies using internal motions. *Robotics and Automation, IEEE Transactions on*, 11(1):139–146, January 1995.

[19] K. Yamada. Arm path planning for a space robot. In *IEEE/RSJ International Conference on Intelligent Robots and Systems*, 1993.